

STATIONARY ACCRETION DISKS LAUNCHING SUPER-FAST-MAGNETOSONIC MAGNETOHYDRODYNAMIC JETS

JONATHAN FERREIRA¹ AND FABIEN CASSE²

Received 2003 November 6; accepted 2003 December 4; published 2004 January 26

ABSTRACT

We present self-similar models of resistive viscous Keplerian disks driving nonrelativistic MHD jets and becoming super-fast-magnetosonic. We show that in order to obtain such solutions, the thermal pressure must be a sizeable fraction of the poloidal magnetic pressure at the Alfvén surface. These steady solutions that undergo a recollimation shock causally disconnected from the driving engine account for structures with a high-temperature plasma in the sub-Alfvénic region. We suggest that only unsteady outflows with typical timescales of several disk dynamical timescales can be produced if the suitable pressure conditions are not fulfilled.

Subject headings: accretion, accretion disks — galaxies: jets — ISM: jets and outflows — MHD — stars: pre-main-sequence

On-line material: color figures

1. INTRODUCTION

Self-collimated jets are now commonly observed originating from young stellar objects (YSOs), active galactic nuclei, and galactic binaries (Livio 1997). All these flows share common properties such as being always correlated with the accretion phenomenon (Hartigan, Edwards, & Ghandour 1995; Falcke & Biermann 1996; Serjeant et al. 1998; Gallo, Fender, & Pooley 2003). It has long been identified that jet self-confinement requires the presence of a large-scale magnetic field in order to focus the outflowing plasma (Chan & Henriksen 1980). The “universal” paradigm of jet formation relies on the occurrence of bipolar magnetic fields threading the accretion disk. As a consequence, the theory of accretion disks had to be revisited in order to take into account the mass, angular momentum, and energy extractions achieved by the jet. One notorious modification to the standard picture is the necessary radial stratification of the disk accretion rate, namely, $\dot{M}_a \propto r^\xi$ (ξ being a measure of the disk ejection efficiency). For instance, $\xi = 0$ describes a standard disk with no outflow, while $0 < \xi < 1$ stands for an ejecting Keplerian accretion disk (Ferreira 1997). If one wishes to obtain the exact ejection efficiency, one has to solve without any approximation the full MHD two-dimensional structure of the disk.

Anomalous magnetic diffusivity must be present within the disk to allow accreting (and rotating) mass to cross the magnetic field lines whereas ejected mass becomes frozen into the field. Only self-similar solutions taking into account the underlying resistive accretion disk hitherto provided this description (Ferreira & Pelletier 1995; Ferreira 1997; Casse & Ferreira 2000a, 2000b). Within these solutions, once in ideal MHD regime, mass is magnetically accelerated along each field line and must successively cross three MHD critical points, namely, the slow and fast magnetosonic (SM and FM) ones and the Alfvénic point. So far, none of the self-similar solutions was able to obtain both disk and jet flows, the latter crossing the three critical surfaces.

Using the same framework, Vlahakis et al. (2000) solved the ideal MHD jet equations and provided new solutions

crossing these three critical points. However, since these solutions were not connected to the underlying disk, the issue of super-FM jet production from the accretion disk remained. In this Letter, we present the necessary conditions to get self-similar super-FM jets (§ 2), discuss the properties of typical solutions (§ 3), and conclude with some astrophysical implications that may be put to the test of observations.

2. ROLE OF A SUB-ALFVÉNIC HEATING

Stationary jets are described by a set of axisymmetric ideal MHD equations. Thus the poloidal magnetic field writes $\mathbf{B}_p = (\nabla a \times \mathbf{e}_\phi)/r$, where $a(r, z) = Cst$ describes a surface of constant magnetic flux. Disk winds are produced whenever a large-scale magnetic field, close to equipartition with the disk thermal pressure (Ferreira & Pelletier 1995), is present over a range in anchoring radii r_0 . The corresponding jet is made of magnetic surfaces nested one around each other with several integrals of motion. In the nonrelativistic case, one gets (u_p poloidal velocity, Ω angular velocity, and ρ density) (1) the mass-to-magnetic flux ratio $\eta(a)$ with $\mathbf{u}_p = \eta(a)\mathbf{B}_p/\mu_0\rho$, (2) the angular velocity of a magnetic surface $\Omega_*(a) = \Omega - \eta B_\phi/\mu_0\rho r$, and (3) the specific total angular momentum $L(a) = \Omega_* r_\lambda^2 = \Omega r^2 - rB_\phi/\eta$ transported away. Here, r_λ is the Alfvén radius where mass reaches the Alfvén poloidal velocity. In this Letter, we are interested in jets that may be heated by their surroundings so that an adiabatic description is inadequate. Instead, we assume the presence of a heat flux $\mathbf{q} = \nabla H - \nabla P/\rho$, where H is the usual enthalpy for a perfect gas. Including this additional effect, one gets the generalized Bernoulli invariant $E(a) + \mathcal{F}(s, a) = (u^2/2) + H + \Phi_G - r\Omega_* B_\phi/\eta$, where $\mathcal{F}(s, a) = \int_{s^+}^s \mathbf{q} \cdot \mathbf{e}_\parallel ds'$ is the heating term that depends on a curvilinear coordinate s along a given magnetic surface (s^+ is roughly the SM point and $\mathbf{B}_p = B_p \mathbf{e}_\parallel$). The total specific energy provided at the disk surface is $E(a) \approx \Omega_0^2 r_0^2 (\lambda - 3/2)$ for a thin disk, where Ω_0 is the Keplerian rotation at the anchoring radius r_0 and $\lambda = L/\Omega_0 r_0^2$ is the magnetic lever arm. The shape of the magnetic surface is given by the Grad-Shafranov (GS) equation

$$(1 - m^2)J_\phi = J_\lambda + J_k + J_\beta, \quad (1)$$

¹ Laboratoire d’Astrophysique de Grenoble, 414 Rue de la Piscine, BP 53, F-38041 Grenoble, France; ferreira@obs.ujf-grenoble.fr.

² Institute for Plasma Physics Rijnhuizen, P.O. Box 1207, 3430 BE Nieuwegein, Netherlands; fcasse@rijnh.nl.

where

$$J_\lambda = \rho r \left[\frac{d\mathcal{E}}{da} + (1-g)\Omega_* r^2 \frac{d\Omega_*}{da} + g\Omega_* \frac{d\Omega_* r_A^2}{da} \right],$$

$$J_\kappa = r \frac{B_\phi^2 - m^2 B_p^2}{2\mu_0} \frac{d \ln \rho_A}{da} + m^2 \frac{\nabla a}{\mu_0 r} \nabla \ln \rho,$$

and

$$J_\beta = \frac{\rho}{B_p} (\nabla \mathcal{F} - \mathbf{q}) \cdot \mathbf{e}_\perp.$$

Here, $\mathbf{e}_\perp = \nabla a / |\nabla a|$, $m = u_p / V_{A,p}$ is the Alfvénic Mach number, and $g = 1 - \Omega / \Omega_*$. The GS equation provides $a(r, z)$ for a given set of invariants. Unfortunately, it is a partial differential equation of mixed type: it is hyperbolic between the cusp [where $u_p = V_c = C_s V_{A,p} / (C_s^2 + V_A^2)^{1/2}$] and the SM surface (where $u_p = V_{SM,p}$), elliptic between the SM and the FM surface (where $u_p = V_{FM,p}$), and hyperbolic farther out. The magnetosonic phase speeds involved in these definitions are the usual ones, i.e., waves traveling along the poloidal field. Solving equation (1) remains a major challenge in applied mathematics: it would require us to a priori know the locus of these surfaces, whereas they emerge as the global solution evolves. In practice, one either solves the time-dependent problem with full MHD codes or uses a method of variable separation.

Self-similar solutions allow us to solve the full set of MHD equations without any approximation. The problem reduces to propagate the solution along a self-similar variable $x = z/r$, which involves the inversion of a matrix. Its determinant vanishes at three singular points where the following numbers become equal to unity: $M_{SM} = V / V_{SM,n}$, $M_A = V / V_{A,n}$, and $M_{FM} = V / V_{FM,n}$, where $V = \mathbf{u}_p \cdot \mathbf{n}$ and $V_{A,n} = V_A \cdot \mathbf{n}$ are projections in the direction \mathbf{n} (see Fig. 1) and $V_{SM/FM,n}^2 = \frac{1}{2} \{ V_A^2 + C_s^2 \pm [(V_A^2 + C_s^2)^2 - 4C_s^2 V_{A,n}^2]^{1/2} \}$ (Ferreira & Pelletier 1995). Not all of these critical points coincide with the above-mentioned points where the flow changes type: $M_A = m$, $M_{SM} \approx u_p / V_c \approx u_p / V_{SM,p}$ (in the cold Keplerian limit), but $M_{FM} < n = u_p / V_{FM,p}$. The critical FM surface is always located downstream in the hyperbolic region. The necessary conditions to provide cold super-Alfvénic (super-A) jets from Keplerian disks were given in Ferreira (1997). Once fulfilled, a super-A solution propagates farther away until collimation by the hoop-stress takes place. This produces an unavoidable decrease of the projected velocity ($V \rightarrow -u_r \approx 0$), even if the poloidal velocity reaches its asymptotic value of $\Omega_0 r_0 (2\lambda - 3)^{1/2}$. The only way to allow for a super-FM solution with $M_{FM} > 1$ is to lower this projection effect by forcing the magnetic surfaces to remain wide open, namely, bringing the Alfvén surface closer to the disk (increase Ψ_A).

The self-similar expression of the GS equation in the cold regime can be written as $\cos \theta_A = R(\theta_A; \Psi_A)$ at the Alfvén point (Casse & Ferreira 2000a). It is an implicit equation providing the jet opening angle θ_A for a given position of the Alfvén surface Ψ_A . In the cold limit, one has $\tan \theta_{SM} \sim \tan \Psi_A (1 - \lambda^{-1/2})$ for a given magnetic lever arm $\lambda \approx r_A^2 / r_0^2$ and initial opening angle θ_{SM} (see Fig. 1). This initial opening angle is constrained by the underlying disk vertical equilibrium. The larger the angle, the larger the magnetic compression and the less mass is being ejected. Only angles up to $\sim 45^\circ$ ($z_A \sim r_A$) have been proved to be possible from Keplerian accretion disks, either with isothermal (Ferreira 1997) or adiabatic jets (Casse

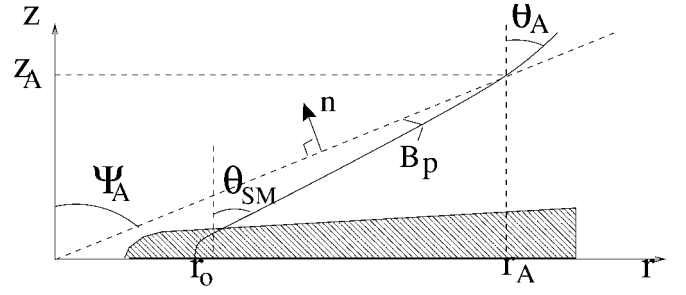


FIG. 1.—Geometry of a disk-wind configuration and definitions of quantities related to the Alfvén critical surface. The unit vector \mathbf{n} is defined as $(z, r) / (r^2 + z^2)^{1/2}$.

& Ferreira 2000a), but none of these solutions can become super-FM.

Every super-FM solution obtained by Vlahakis et al. (2000) exhibits Alfvén surfaces closer to the equatorial plane (i.e., $\Psi_A \sim 60^\circ$), but being not connected to a resistive MHD disk, they did not have to fulfill the requirement of a quasi-static disk vertical equilibrium. Actually, no Keplerian disk would probably survive the overwhelming magnetic compression imposed by the bending of the field lines (or allow the imposed mass effluvium). The only possible way to have an Alfvén surface closer to the disk is to break this univocal link between Ψ_A and θ_{SM} . This implies a change of some invariants (entropy and total specific energy) between the disk and the Alfvén surface. Physically this requires an extra force term in the GS equation, namely, a strong outwardly directed pressure gradient in the sub-A region. Within the self-similar framework, it means building up a large thermal pressure, thus an additional heating starting above the disk.

The generalized GS equation becomes $\cos \theta_A = R(\theta_A; \Psi_A) + R_\beta(\theta_A; \Psi_A)$, where

$$R_\beta(\theta_A; \Psi_A) = -\frac{g_A \beta_A}{4} \left[\frac{2}{g_A} \cos \theta_A + \frac{\sin \Psi_A}{\sin(\Psi_A - \theta_A)} \right]$$

$$\times \left(\frac{\mathcal{F}_A}{C_{s,A}^2} - \frac{2}{g_A} - \frac{d \ln \rho_A}{d \ln r_0} - \frac{1}{\gamma - 1} \right)$$

$$+ \frac{\cos(\Psi_A - \theta_A)}{\sin \Psi_A} \left(\frac{r_A \mathbf{q} \cdot \mathbf{e}_{\parallel A}}{C_{s,A}^2 \cos \theta_A} - \left| \frac{\partial \ln C_s^2}{\partial x} \right|_A \right) \quad (2)$$

is the contribution of this additional heat flux and β_A is the ratio of the plasma pressure $P_A \equiv \rho_A C_{s,A}^2$ to the poloidal magnetic pressure at the Alfvén point. This equation shows that β_A large enough ($\beta_A \lesssim 1$) and R_β negative are two necessary conditions to increase Ψ_A . Indeed, since θ_A is always smaller than Ψ_A , any tendency to increase θ_A leads to a lowering of the Alfvén surface.

At the Alfvén surface, $\beta_A = 2\omega_A^2 (\epsilon^2 / \lambda) (T_A / T_0)$, where $\omega_A = \Omega_* r_A / u_{p,A} \geq 1$ (Ferreira 1997; Casse & Ferreira 2000a) and $\epsilon = h/r$ is the disk aspect ratio. This general expression shows that any cold jet (isothermal $T_A = T_0$ or adiabatic $T_A \ll T_0$) always displays $\beta_A \ll 1$. In order to have any influence on the transverse equilibrium, this additional heating must provide a large increase in jet temperature, namely, $T_A \geq T_0 / \epsilon^2$. The second condition ($R_\beta < 0$) sheds light on the required heat-

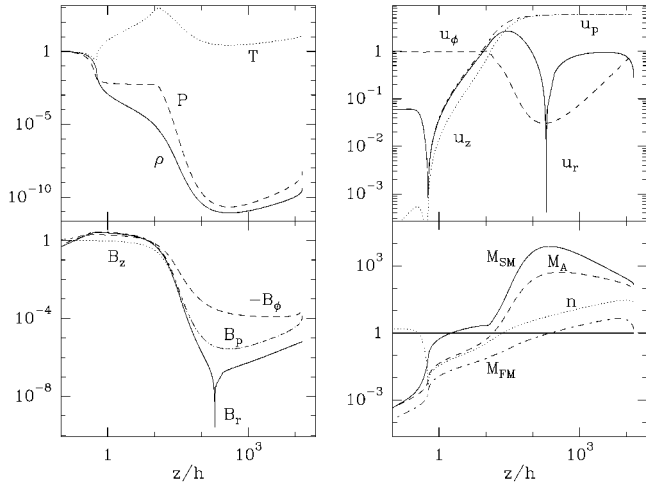


FIG. 2.—Typical super-FM disk wind with $\xi = 0.03$ and $\epsilon = 0.03$ ($h = \epsilon r$). Density, pressure, and temperature are normalized to their value at the disk midplane, the magnetic field components to $B_z(z = 0)$, and the velocities to the Keplerian speed at the anchoring radius r_0 . All magnetic field components remain comparable from the disk surface to the Alfvén point. Note that the density profile inside the disk, where both u_r and u_z are negative, is very different from a Gaussian. Recollimation takes place at $z \approx 3 \times 10^3 r_0$. [See the electronic edition of the Journal for a color version of this figure.]

ing function. The sum of the first two terms in equation (2) is usually always negative. Indeed, energy conservation gives $\mathcal{F}_A/C_{s,A}^2 \geq (\gamma/\gamma - 1) [1 - (T_0/T_A)]$ because of the tremendous cooling due to the jet expansion. Since T_A must be large, the ratio $\mathcal{F}_A/C_{s,A}^2$ is always large enough (but of the order of unity). The third term of equation (2) shows that the most favorable situation is the presence of additional heating mainly in the sub-A region, i.e., a vanishing heat flux ($\mathbf{q} \cdot \mathbf{e}_{\parallel A} = 0$ or very small) and an already decreasing temperature (due to adiabatic cooling).

3. SELF-SIMILAR NUMERICAL SOLUTIONS

We follow basically the same integration procedure as in our previous works (see Casse & Ferreira 2000b for more details). A heating function is assumed to be present, starting at the disk surface but vanishing before the Alfvén point, with an adiabatic index $\gamma = 5/3$. Further up, we allow for a continuous transition to a polytropic energy equation, $P \propto \rho^\Gamma$. The X-type FM critical point allows to determine the critical value Γ_c of the polytropic index: if $\Gamma < \Gamma_c$, thermal acceleration is too inefficient (breezlike solution), whereas if $\Gamma > \Gamma_c$, the strong decrease in enthalpy leads to a shocklike solution. Although Vlahakis et al. (2000) used an analogous way, our solutions strongly differ by the fact that jet invariants are fixed by the disk. Therefore, we need first to drastically increase the jet enthalpy before fine-tuning the polytropic index. As in solar wind models, we are playing around with one free parameter (Γ) while one should solve the full energy equation.

Figure 2 shows a typical super-FM solution obtained with $\Gamma_c = 1.45$. The energy input required can be measured by the ratio $f = \mathcal{F}(x_A, a)/E(a)$ since most of the heating occurs in the sub-A region. Solutions displayed here required f of several 10^{-3} , allowing us to get $\Psi_A \approx 65^\circ$ with $\beta_A \approx 0.1$ (condition $T_A \sim T_0/\epsilon^2$ is verified). Note that smaller temperature values would also allow super-FM jets, but they would just be terminated much sooner as in Vlahakis et al. (2000).

In general two-dimensional flows, the “causal horizon” (here the $M_{FM} = 1$ surface) is the envelope of one of the two families

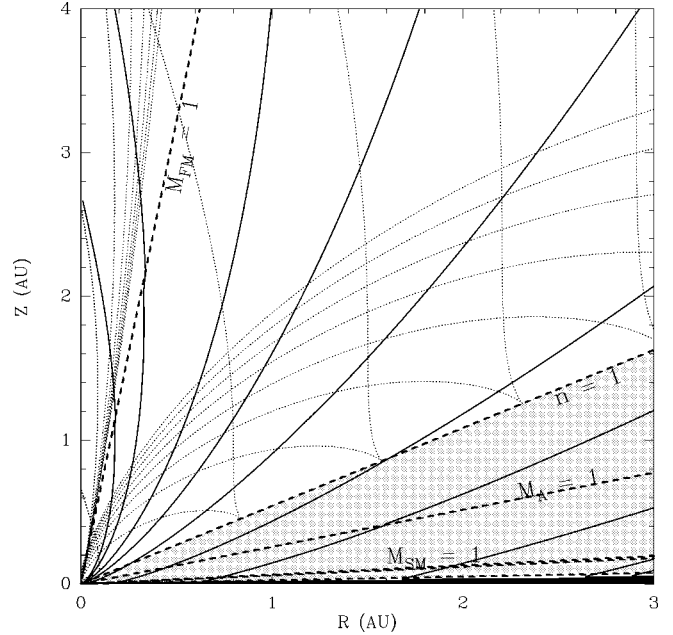


FIG. 3.—Poloidal cross section showing the three critical surfaces (SM, A, and FM) and some characteristics (dotted lines, the hyperbolic domain), as well as the two elliptic regions (shaded). Contrary to Vlahakis et al. (2000), the streamlines (solid lines) are computed from the midplane of the resistive accretion disk. This solution has $\xi = 0.09$, $\epsilon = 0.03$, and $\Gamma_c = 1.56$. [See the electronic edition of the Journal for a color version of this figure.]

of characteristics (Tsinganos et al. 1996) and not the surface of parabolicity $n = 1$ (see Fig. 3). Any perturbation occurring to the flow downstream to the $M_{FM} = 1$ surface is unable to cross this horizon. This result is generic to two-dimensional solutions; the only bias introduced by self-similarity is the conical shape of such surfaces, not their separate existence. This has strong consequences on numerical experiments, as already pointed out by Ustyugova et al. (1999). To ensure the absence of feedback from the imposed boundary conditions, the Mach cones (defined locally as the tangents to the characteristics) must be directed out of the computational domain at its boundaries.

4. ASTROPHYSICAL IMPLICATIONS

The present computed MHD flows are the first-ever steady state solutions describing an overall accretion-ejection structure from the resistive accretion disk to the super-FM jet region. The strict stationarity of such accretion-ejection engines depends critically on the thermal properties of the sub-A region. If the plasma pressure, measured at the Alfvén point, is a sizable fraction of the poloidal magnetic pressure, MHD jets from Keplerian accretion disks can become super-FM. In the super-FM region, the jet is always facing a recollimation that ends up as a shock. The further jet propagation requires numerical time-dependent simulations. Around a protostar, such thermal pressure gradient occurs whenever temperatures as high as several 10^5 K are reached along the inner streamline. This is compatible with recent observations of blueshifted UV emission lines (Gómez de Castro & Verdugo 2001) and some absorption features (Takami et al. 2002). Unfortunately, the heating source can only be inferred from its effects, and its origin remains a crucial issue. For instance, YSOs’ accretion disks are assumed to be highly magnetized, so one may safely expect that some accretion energy is also dissipated in the upper disk layers and

provides coronal heating (Galeev, Rosner, & Vaiana 1979; Heyvaerts & Priest 1989). This is actually shown by both numerical simulations (Miller & Stone 2000) and some observational indication of accretion-powered coronae (Kwan 1997). Moreover, since the central object has a hard surface, the shock of the infalling material provides another source of UV radiation (as well as X-rays), illuminating the disk and heating the sub-A region (Ferro-Fontán & Gómez de Castro 2003). An alternative to this additional heating would be the presence of a high-pressure inner flow (a “spine”) forcing the MHD disk wind to open up. In YSOs such a flow could be provided by the interaction between the protostellar magnetosphere and the disk (Ferreira, Pelletier, & Appl 2000; Matt et al. 2002; Romanova et al. 2002). Temperatures required around a compact object imply a relativistic plasma. In this case, the inner pressure could be provided by an inner beam composed of relativistic electron-positron pairs, heated and accelerated inside the hollow part of the disk wind (Renaud & Henri 1998).

On the other hand, if an accretion-ejection engine cannot provide this additional heating or if there is no inner spine, then the thermal pressure is negligible at the Alfvén surface and jets remain sub-FM. Recollimation toward the axis leads to the formation of a shock, and the overall structure is therefore unsteady. However, no MHD signal can propagate upstream along the magnetic field toward the disk. Instead, in this hyperbolic region, the information that a shock has occurred is first carried away by MHD waves traveling along the characteristics until the $n = 1$ surface is reached (see Fig. 3). Once in the elliptic domain, the fastest mode travels along the magnetic field down to the disk. As a consequence, the time taken by MHD waves to inform the disk is always larger than the one given by, for example, computing the time $\tau =$

$\int ds/V_{\text{FM},p}$ taken by the fast mode along the same field line. As an illustration, let us take the cold sub-FM solutions of Ferreira (1997), as pictured in his Figure 6. For the solutions recollimating right after the Alfvén surface, this time τ is roughly equal to the orbital period τ_0 at the anchoring radius, whereas for those recollimating much farther away, one gets $\tau \geq 10^2 \tau_0$. The presence of sporadic jet events with timescales much larger than disk dynamical timescales (Raga et al. 2002; Gallo et al. 2003 and references therein) could fit into the picture of an accretion-ejection engine trying to adjust itself.

The amount of large-scale poloidal magnetic flux trapped in accretion disks is completely unknown. The above astrophysical implications hold only if this flux is large enough so that an equipartition field spans at least one decade in radius in the disk. Indeed, in such circumstances, there is no physical reason for strong gradients in jets, and one may expect an almost plane Alfvén surface (Krasnopolsky, Li, & Blandford 1999; Casse & Keppens 2004). These kind of jets display dynamical properties (acceleration and collimation) that weakly depend on the radial (inner and outer) boundary conditions, as in self-similar models. On the contrary, if the flux is small and concentrated at the inner edge of the disk, one would expect an almost spherical expansion of the field lines as in X-wind models (Shu et al. 1994). Observations allowing to infer jet velocity patterns and to relate them to the source (Garcia et al. 2001; Bacciotti et al. 2002; Pesenti et al. 2003) are necessary to discriminate between these two extreme pictures.

F. C. is a postdoctoral fellow of the European Community’s Human Potential Programme PLATON under contract HPRN-CT-2000-00153. F. C. would also like to thank the team SHERPAS for its hospitality during his stay at the LAOG.

REFERENCES

- Bacciotti, F., et al. 2002, *ApJ*, 576, 222
 Casse, F., & Ferreira, J. 2000a, *A&A*, 353, 1115
 ———. 2000b, *A&A*, 361, 1178
 Casse, F., & Keppens, R. 2004, *ApJ*, 601, 90
 Chan, K. L., & Henriksen, R. N. 1980, *ApJ*, 241, 534
 Falcke, H., & Biermann, L. 1996, *A&A*, 308, 321
 Ferreira, J. 1997, *A&A*, 319, 340
 Ferreira, J., & Pelletier, G. 1995, *A&A*, 295, 807
 Ferreira, J., Pelletier, G., & Appl, S. 2000, *MNRAS*, 312, 387
 Ferro-Fontán, C., & Gómez de Castro, A. I. 2003, *MNRAS*, 342, 427
 Galeev, A. A., Rosner, R., & Vaiana, G. S. 1979, *ApJ*, 229, 318
 Gallo, E., Fender, R. P., & Pooley, G. G. 2003, *MNRAS*, 344, 60
 García, P. J. V., Cabrit, S., Ferreira, J., & Binette, L. 2001, *A&A*, 377, 609
 Gómez de Castro, A. I., & Verdugo, E. 2001, *ApJ*, 548, 976
 Hartigan, P., Edwards, S., & Ghandour, L. 1995, *ApJ*, 452, 736
 Heyvaerts, J., & Priest, E. R. 1989, *A&A*, 216, 230
 Krasnopolsky, R., Li, Z. Y., & Blandford, R. 1999, *ApJ*, 526, 631
 Kwan, J. 1997, *ApJ*, 489, 284
 Livio, M. 1997, in *ASP Conf. Ser. 121, Accretion Phenomena and Related Outflows*, ed. D. T. Wickramasinghe, G. V. Bicknell, & L. Ferrario (San Francisco: ASP), 845
 Matt, S., et al. 2002, *ApJ*, 574, 232
 Miller, K. A., & Stone, J. M. 2000, *ApJ*, 534, 398
 Pesenti, N., Dougados, C., Cabrit, S., O’Brien, D., Garcia, P., & Ferreira, J. 2003, *A&A*, 410, 155
 Raga, A. C., et al. 2002, *A&A*, 395, 647
 Renaud, N., & Henri, G. 1998, *MNRAS*, 300, 1047
 Romanova, M. M., Ustyugova, G. V., Koldoba, A. V., & Lovelace, R. V. E. 2002, *ApJ*, 578, 420
 Serjeant, S., et al. 1998, *MNRAS*, 294, 494
 Shu, F., et al. 1994, *ApJ*, 429, 781
 Takami, M., et al. 2002, *ApJ*, 568, L53
 Tsinganos, K., Sauty, C., Surlantzis, G., Trussoni, E., & Contopoulos, J. 1996, *MNRAS*, 283, 811
 Ustyugova, G. V., Koldoba, A. V., Romanova, M. M., Chetchetkin, V. M., & Lovelace, R. V. E. 1999, *ApJ*, 516, 221
 Vlahakis, N., Tsinganos, K., Sauty, C., & Trussoni, E. 2000, *MNRAS*, 318, 417